

PAWDQ: A 3D Printed, Open Source, Low Cost Dynamic Quadruped

Joonyoung Kim¹, Taewoong Kang¹, Dongwoon Song¹, Seung-Joon Yi¹

Abstract— In this paper we present a new open source dynamic quadruped robot, PADWQ (pronounced pa-dook). In contrast to other quadruped robots that are either relying upon custom actuators and machined metal parts, or low-torque, high-gain servomotors that seriously limit the dynamic performance of the robot, the suggested robot consists entirely of 3D printed plastic structural parts and off-the-shelf commercial components, which allows for a rapid duplication, modification and distribution of the robot for various education and research purposes. It has 12 torque controlled quasi-direct drive (QDD) joints with a close loop control rate of 1 kHz, as well as onboard RGBD camera and GPU-equipped perception computer that can map the terrain and detect various objects in front of the robot. Preliminary test results show that the PADWQ is capable of dynamic trot-walking at the speed of 1 meter per second, even with a relatively simple motion controller.

I. INTRODUCTION

Quadruped locomotion has a number of potential advantages over other locomotion types, the biggest of which is the ability to handle uneven terrain. However, commonly used electric motors is not well suited for direct actuation of legged robot joints as they require much higher peak torque than most motors are capable of. Typically, a high-rpm motor is used with a high ratio gear reducer such as the Harmonic drive to generate the high peak torque required for legged robots. However, as such a setup has limited backdrivability, high reflected inertia and low impact resistance, it is not ideal for dynamic locomotion over uneven terrain.

Recent introduction of the quasi-direct drive (QDD) [1], [2], [3], which uses a high-torque motor paired with low ratio gear reducer without an elastic component [4], [3], has brought a number of highly dynamic electric powered quadrupeds with excellent maneuverability comparable to hydraulic powered quadrupeds [5], [6], [7], [8], [9]. In addition, thanks to the big success of the quadrotors that have led to the influx of inexpensive high-performance brushless DC (BLDC) motors, QDD actuators can now be built at a low cost using commercially available off-the-shelf parts [10].

Another recent advance is the widespread adoption of affordable 3D printers, which allows manufacturing of complex 3D parts without relying upon costly processes such as CNC machining. This greatly helped spreading of the open source hardware, where the blueprints and assembly instructions are openly released so that the hardware can be rapidly duplicated and distributed across researchers. There have been a number open source quadruped projects as well,

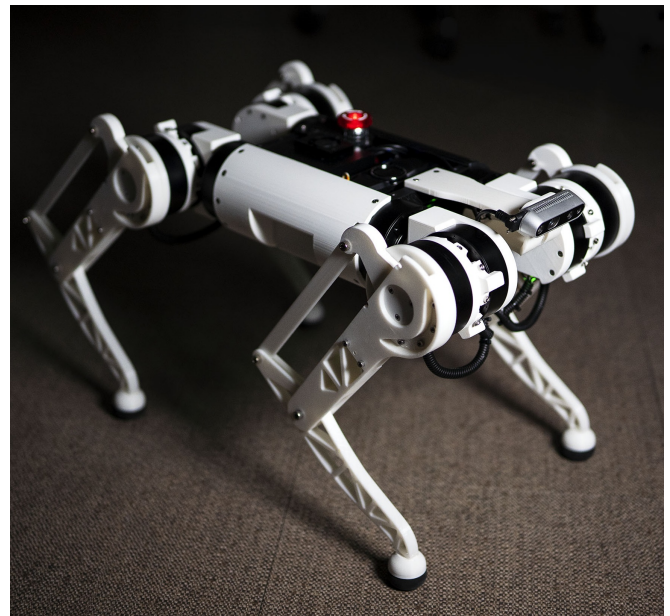


Fig. 1: The PADWQ

but to our knowledge, most of those open source robotic platforms are based on position controlled servo motors [11], [12], [13] which greatly limits their size, performance and possible applications. Two exceptions, the Stanford Doggo [3] and Solo [14], use custom QDD actuators that allows for dynamic behaviors such as jumping, but their real-world application is still limited as they are lightweight, low DOF quadrupeds solely designed for research purposes.

In this paper, we present an open-source dynamic quadruped robot platform that is entirely built upon commercial, off-the-shelf components and standard 3D printed plastic structural parts, so that the robot can be easily duplicated, modified and distributed even without access to advanced machining processes. All the structural parts can be directly 3D printed from openly released STL files, and whole robot can be easily assembled only using hand tools in less than two man hours. The robot has two powerful onboard computers, each handling motion and perception processing, and has torque controlled modular QDD actuators that are capable of dynamic locomotion. Preliminary testing with the assembled robot has showed that the robot is capable of dynamic trot-walking at the velocity of 1.0 meter per second, even with a simple motion controller without extensive parameter tuning, and has expected runtime of one hour using internal batteries.

¹Department of Electrical Engineering, Pusan National University,
Busan, South Korea
{kjyky98, tony1, dongwoon, seungjoon.yi}
@pusan.ac.kr

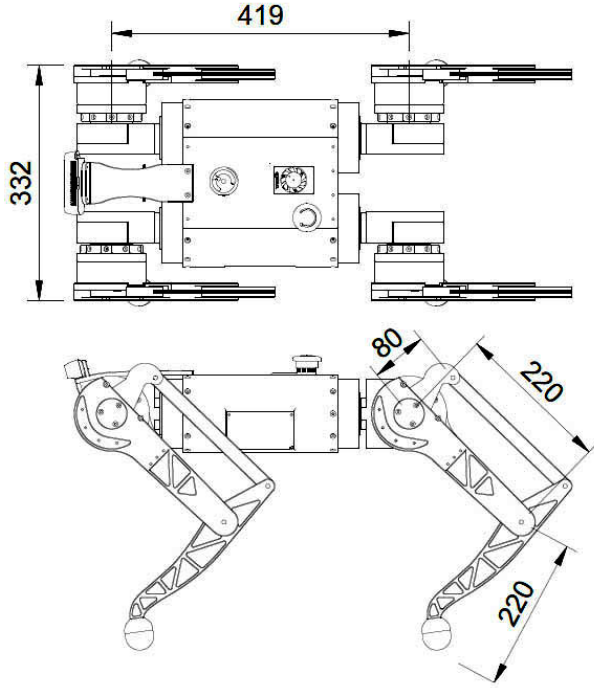


Fig. 2: Overall dimension of the PADWQ

II. HARDWARE DESIGN

The overall design of the PADWQ is largely based on recent quadrupeds based on modular QDD actuators. It has four 3 DOF legs, each of which consists of three serial rotational joints, which are controlled by three modular actuators that are clustered together to lower the leg inertia, and a spherical rubber feet. PADWQ has leg link lengths of 0.22 meters for both the upper and lower links, and 0.419 meter long between the front and rear leg pitch joints, and 0.332 meter wide. The robot weighs 11.7 kg without batteries, and 12.7kg with two batteries for computers and actuators. Compared to the MIT Mini Cheetah, PADWQ is approximately 10 percent larger in every direction and 40 percent heavier, or 5 percent more dense when scaled to the same size.

A. Modular Actuators

1) *Actuator Selection:* Since the introduction of the MIT Mini Cheetah and its low-cost modular actuator based on commercial BLDC motor and planetary gears, a number of brands are now commercially providing a pre-assembled QDD actuator with the same design principle. They all consists of a high-torque BLDC motor, planetary reduction gear located at the center of the actuator, and integrated magnetic encoder and motor driver that allows closed-loop feedback control of the actuator. For this platform, we have chosen the Gyems RMD-X8 series actuators, which is shown with the Mini Cheetah actuator in Fig. 3, as they were available in large quantities at open markets, comes with proper documents and diagnosis software, and most affordable at the time of writing this paper. The RMD-X8

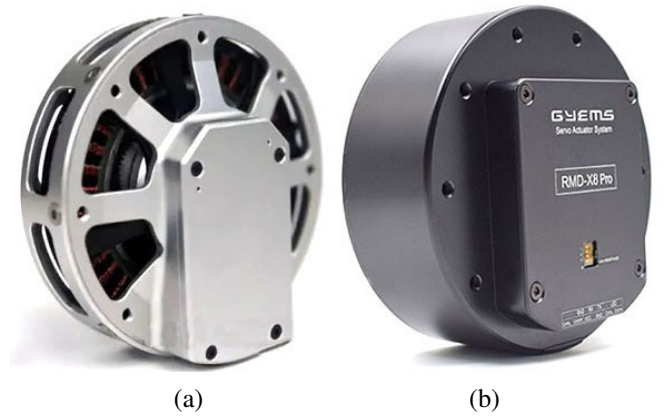


Fig. 3: Comparison of two modular actuators. (a) MIT Mini Cheetah actuator (b) Gyems RMD-X8 series

TABLE I: Comparison of QDD actuators

	Mini Cheetah Actuator	Gyems RMD-X8	Gyems RMD-X8 Pro
Weight (g)	480	620	750
Gear ratio	6:1	6:1	6:1
Nominal Torque (Nm)	6.9	9	12
Peak Torque (Nm)	17	21	35
Torque density (Nm/kg)	35.4	33.9	46.7
Joint Velocity (rad/s)	40	26.2	23.6
Market Price (USD)	\$300 (BOM)	\$359	\$449

series actuators have a number of similarity to the MIT Mini Cheetah actuator, including the outer dimensions, reduction ratio, bus interface and control methods. They have a number of differences as well, which includes a hardware DIP switch for motor ID setting and separate UART port that can be used to diagnose the actuator status and set up various parameters.

Table I compares the official specifications of two RMD-X8 series actuators to the MIT Mini Cheetah actuator. Compared to the Mini Cheetah actuator, both actuators are considerably heavier, mainly due to fully enclosed casing, yet also have higher peak torque. As a result, the torque density of the RMD-X8 actuator is 95.8 percent of the Mini Cheetah actuator, and that of the RMD-X8 pro actuator is 113.9 percent of the Mini Cheetah actuator. Overall, both of the Gyems actuators compares very favorably against the Mini Cheetah actuator on paper, especially considering their retail prices are only slightly higher than the bill of material (BOM) of the Mini Cheetah actuator.

2) *Actuator Testing:* We have run through a number of tests to check the actual properties of the RMD-X8 series actuators. Although the position and velocity based control methods are well explained in the supplied control protocol manual, the manual says that the actuator can be controlled by *torque current*, where it is not clear whether the target control value is the target torque or input current. In addition, the manual does not provide actual coefficient for the control value either, only saying that the bus current and torque output may vary with different actuators. We have measured the relationship between *torque current* control value, input current and output torque using a digital torque sensor and

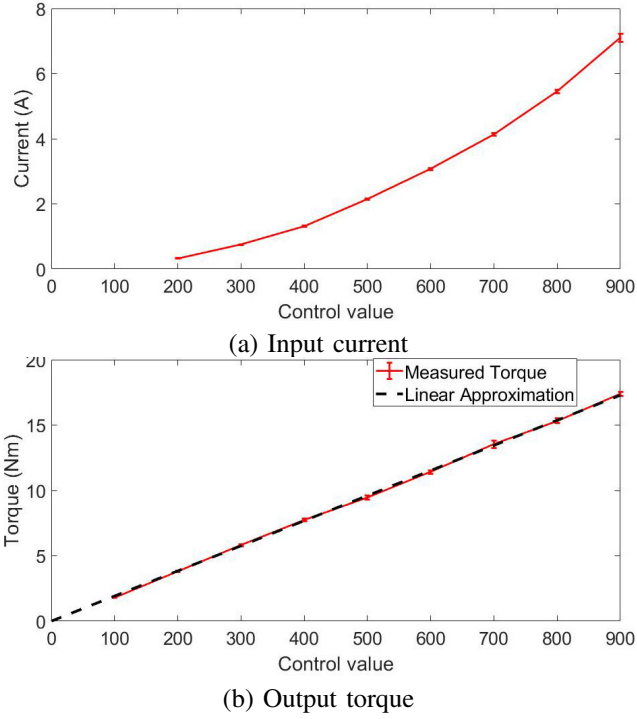


Fig. 4: Relationship between torque current control variable, measured input current and output torque for RMD-X8 actuator

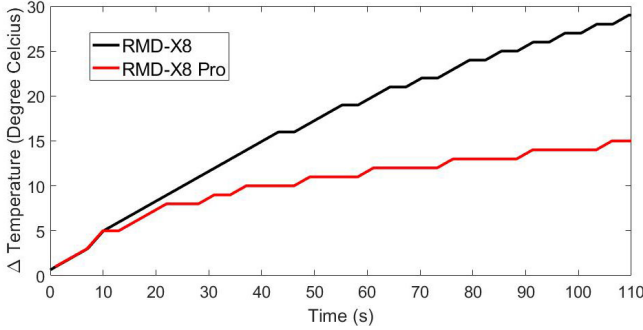


Fig. 5: Temperature rise over time for RMD-X8 and RMD-X8 pro actuators with 9Nm output torque

power analyzer. The result, which is shown in Fig. 4, shows that the *torque current* control variable actually controls the output torque, not the input current. We have used the least square approximation to fit a linear line to the output torque data, where the coefficient is found to be 52.0639.

Finally, we have tested the thermal characteristics of the RMD-X8 series actuator over time. The internal temperature of the actuators are measured using the built in thermal sensor, while generating a constant torque of 9 Nm, the nominal torque of the RMD-X8 actuator. We have found that internal temperature rise is approximately 30 degree Celsius for RMD-X8 actuator and 15 degree Celsius for RMD-X8 pro actuator after 110 seconds of testing.

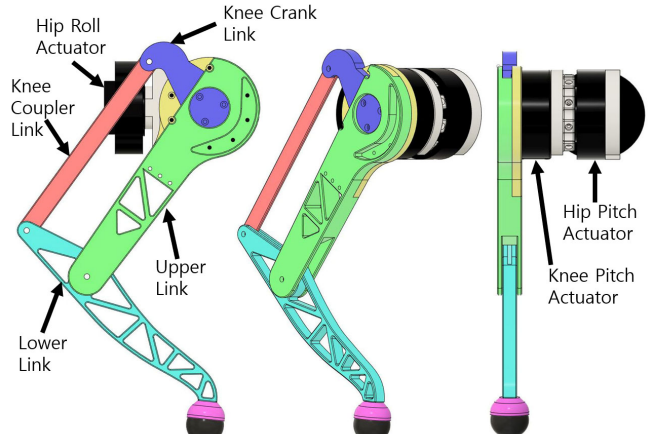


Fig. 6: 3DOF Leg with a parallelogram linkage

B. Leg Design

Our 3 DOF design is designed to minimize the limb inertia for highly dynamic locomotion, while leveraging now ubiquitously available 3D printing process. We have followed common design approach to minimize the limb inertia, where all limb actuators are closely located near the center of the hip joint and the knee joint is actuated remotely. Typical ways to actuate knee joint remotely includes the four-bar linkage [12], [15], [16], timing belt [10], [17] and roller chain [18]. Although the timing belt and roller chain mechanisms allow for wider joint range of motion and the ability to add more gear reduction, such as 1.55:1 knee gear reduction of the Mini Cheetah, we have chosen the parallelogram linkage design, as the whole mechanism is simpler and can be fully 3D printed. To handle the higher torque load and accompanying heat buildup of the knee actuator without using additional gear reduction, we use stronger RMD-X8 pro actuator for the knee joint and lighter RMD-X8 actuator for hip roll and pitch joints.

Fig. 6 shows the leg design. The range of motion for the knee joint, which is limited by the four bar linkage mechanism, is -134° to -7° . We use additional mechanical joint stops to prevent cable damage due to the overrotation, which limits the range of motion of hip roll joint to be -30° to 30° and that of hip pitch joint to be -51° to 93° .

C. Torso Design

Torso houses various electronics components that includes batteries, control computers, IMU and wireless receiver, which are shown in Fig. 7. We use two onboard computers to handle the motion control and perception loads separately. A LattePanda Alpha single board computer with powerful Intel core-M3 8100Y CPU, 8GB RAM and 256GB of NVMe storage is used for motion control of the robot. We have chosen a very fast motion control PC for futureproofing, which has CPU with almost four times faster single thread performance and storage with 40 times writing speed compared to the Intel Atom based SBC used in [10]. Perception load is handled by a NVidia Xavier Jetson NX single board computer, which has 384 CUDA cores that can run deep learning based

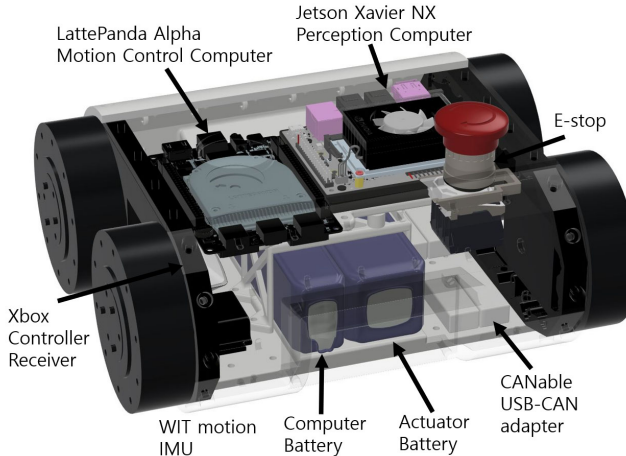


Fig. 7: Torso components

TABLE II: Summary of 3D printing results

Part name	Qty.	Material used(g)	Printing time(hr)
Hip Interface Link	4	251	15.9
Knee Crank Link	4	54	3.1
Knee Coupler Link	4	19	1.2
Leg Upper Link	4	199	13.4
Leg Lower Link	4	82	5.9
Foot Mount	4	4	0.3
Torso Side Plate	2	233	19.0
Torso Bottom Plate	1	10	10
Torso Top Plate	1	81	5.1
Torso Leg Mount	2	51	4.8
Realsense Mount	1	61	5.5

computationally heavy perception algorithms in real time. Two computers are connected via Ethernet connection, and communicates using the ROS middleware. Four CANable open-source USB to CAN adapter are connected to the motion control computer, one per each leg, so that all actuators can be controlled at the close-loop control rate of 1 kHz. WIT WTC901C IMU and Xbox wireless receiver are also connected to the motion control computer.

We have tested two power options for the robot. The first option uses a single 6-cell, 222 Wh LiPo battery, which directly powers the actuators and uses 12V step-down converter to power two onboard computers, and the second option uses two separate batteries, a 3-cell 58 Wh battery for computers and a 6-cell 93 Wh battery for actuators. For both power options, batteries are loaded sideways to the battery compartment space located at the bottom center of the torso. We have found that the average power consumption of two computers under full loads to be approximately 35W, which translates into one hour and forty minutes of runtime in the worst case.

III. MANUFACTURING AND ASSEMBLY

We have used two hobbyist grade 3D printers, QIDI X-Max and FlashForge Creator 3, to print all the structural parts. We have used commonly available PLA material for printing all the parts, and the nozzle travel speeds are set to 100 mm/s for both printers. Table II summarizes the

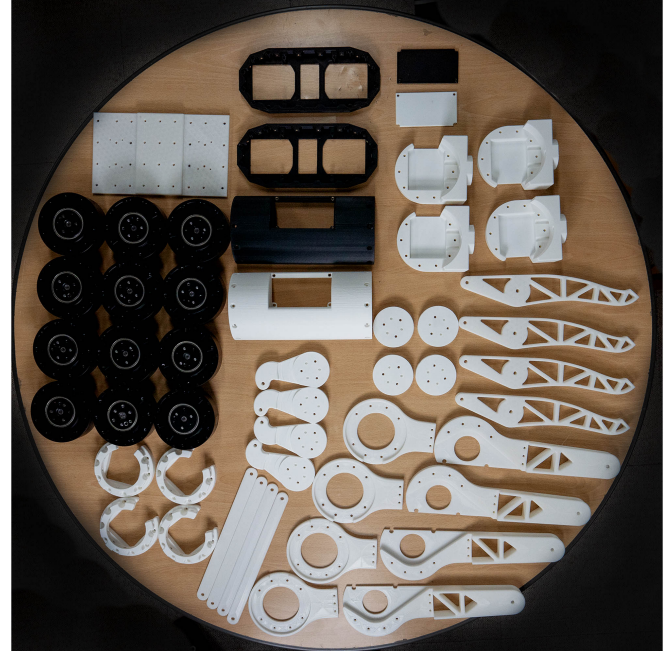


Fig. 8: 3D printed parts of PADWQ before assembly

TABLE III: Price Breakdown of PADWQ

Component	Unit Price (USD)	Qty	Total Price (USD)
RMD-X8 Actuator	359	12	4308
RMD-X8 Pro Actuator	448	4	1792
Lattepanda Alpha	399	1	425
Jetson Xavier NX	399	1	399
WIT WTC901C IMU	34	1	34
XBOX 360 receiver	24	1	24
CANable USB-CAN	39	4	156
RealSense D435	170	1	170
6s 4200mAh Battery	120	1	120
3s 5200mAh Battery	68	1	68
3D Printing Material	30	3.2	96
Others	100	1	100
Total			7692
Total w/o Perception			7123

material used and time spent for printing for each part. It takes approximately 220 hours of printing time and 3.2kg of the printing material to print all the structural parts, which actually took around 5 days as two printers have been used in parallel. STL files of all the structural parts are released as open source in [19].

The assembly of the robot is rather straightforward as all the parts are held together by standard hex bolts and nuts. Assembly only requires hand tools, and it takes less than two man hours to fully assemble the robot from the individual parts shown in Fig. 8.

IV. MOTION CONTROL

We have used a simple motion control structure, which is based on our previous software framework used for position controlled bipedal robots [cite], to test the basic capability of the system. At the lowest level, we run four separate leg communication processes, which handles close loop control of a single leg chain using a simple PD control. Each process

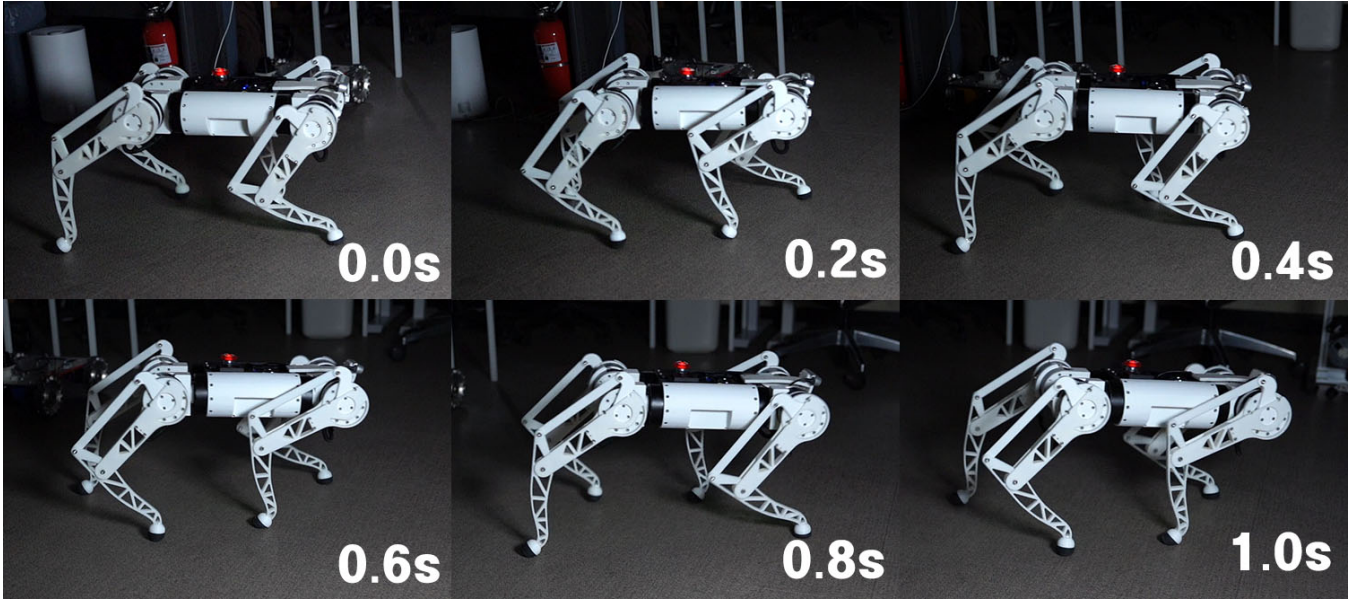


Fig. 9: Dynamic trot-walking of PADWQ at 1.0m/s



Fig. 10: Continuous walking experiment

receives current actuator positions and velocities, calculates the control torques using the PD control law, and sends the control torques to the actuators at the rate of 1 kHz. The target joint angles are updated at the trajectory controller, which uses cubic spline function and linear inverted pendulum model to generate the feet and torso trajectories at every step, and calculate the corresponding leg joint angles using the inverse kinematics of the robot. At the highest level, the target torso pose and leg positions are determined at the beginning of each step period, using their current values and the command velocity from a human operator. The motion control structure can generate a number of different gait patterns by simply changing the swing foot patterns, which includes crawl, trot, pace and bound gaits. We plan to adopt advanced quadruped motion control methods, such as a real-time model predictive control [20], in the future.

V. EXPERIMENTAL RESULTS

We have done a preliminary locomotion test using the PADWQ, and we have found the robot can reliably perform



Fig. 11: Actuator temperature after 50 minutes of continuous walking

a dynamic trot-walking over various surfaces, even with a simple motion controller without extensive parameter tuning. The maximum walk speed measured during the test is 1.0 m/s, as shown in Fig. 9. To test the power consumption and long term integrity of the robot, we have performed a continuous walking experiment which let the robot continuously walk in place. After 50 minutes of testing, we have found the peak and average power consumption to be 188W and 81.6 W, respectively. Fig. 11 shows the FLIR image of leg actuators after the experiment. The knee actuator temperature has risen by 21.5 degree Celsius to reach the final temperature of 46.5 Degree Celsius after the 50 minutes of locomotion, which is quite lower than the glass transition temperature of the PLA material used for the robot. If we

extrapolate the power and temperature measurement values, we can conclude that the PADWQ can safely operate for one full hour using the internal power source.

VI. CONCLUSIONS

In this paper, we present a 12.7kg open source quadruped that is entirely made of commercial off-the-shelf components and standard 3D printed plastic structural parts for quick duplication, modification and distribution for various purposes. Unlike previous open source quadrupeds that are based on position controlled servomotors or low-torque custom actuators, the suggested robot uses powerful modular QDD actuators that allow for advanced torque-based control methods. Preliminary test with a simple motion controller shows that the quadruped is capable of highly dynamic maneuvers, and can reliably operate for one hour using internal battery.

ACKNOWLEDGEMENTS

This work was partially supported by Institute of Information & communications Technology Planning & Evaluation (IITP) grant funded by the Korea government (MSIT) (No. 2018-0-00622) and the National Research Foundation of Korea(NRF) grant funded by the Korea government(MSIT) (No.2019R1F1A1063846).

REFERENCES

- [1] S. Seok, A. Wang, D. Otten, and S. Kim. Actuator design for high force proprioceptive control in fast legged locomotion. In *2012 IEEE/RSJ International Conference on Intelligent Robots and Systems*, pages 1970–1975, 2012.
- [2] P. M. Wensing, A. Wang, S. Seok, D. Otten, J. Lang, and S. Kim. Proprioceptive actuator design in the mit cheetah: Impact mitigation and high-bandwidth physical interaction for dynamic legged robots. *IEEE Transactions on Robotics*, 33(3):509–522, 2017.
- [3] N. Kau, A. Schultz, N. Ferrante, and P. Slade. Stanford doggo: An open-source, quasi-direct-drive quadruped. In *2019 International Conference on Robotics and Automation (ICRA)*, pages 6309–6315, 2019.
- [4] W. Bosworth, S. Kim, and N. Hogan. The mit super mini cheetah: A small, low-cost quadrupedal robot for dynamic locomotion. In *2015 IEEE International Symposium on Safety, Security, and Rescue Robotics (SSRR)*, pages 1–8, 2015.
- [5] Hae-Won Park and Sangbae Kim. Quadrupedal galloping control for a wide range of speed via vertical impulse scaling. *Bioinspiration & Biomimetics*, 10(2):025003, mar 2015.
- [6] Hae-Won Park, Patrick M Wensing, and Sangbae Kim. High-speed bounding with the mit cheetah 2: Control design and experiments. *The International Journal of Robotics Research*, 36(2):167–192, 2017.
- [7] J. Hooks, M. S. Ahn, J. Yu, X. Zhang, T. Zhu, H. Chae, and D. Hong. Alphred: A multi-modal operations quadruped robot for package delivery applications. *IEEE Robotics and Automation Letters*, 5(4):5409–5416, Oct 2020.
- [8] P. Wensing H.-W. Park and S. Kim. Online planning for autonomous running jumps over obstacles in high-speed quadrupeds. *Proceedings of the 2015 Robotics: Science and Systems Conference*, pages 1–9, July 2015.
- [9] H. Park, Sangin Park, and S. Kim. Variable-speed quadrupedal bounding using impulse planning: Untethered high-speed 3d running of mit cheetah 2. In *2015 IEEE International Conference on Robotics and Automation (ICRA)*, pages 5163–5170, 2015.
- [10] B. Katz, J. D. Carlo, and S. Kim. Mini cheetah: A platform for pushing the limits of dynamic quadruped control. In *2019 International Conference on Robotics and Automation (ICRA)*, pages 6295–6301, 2019.
- [11] F. García-Cárdenas, N. Soberón, O. E. Ramos, and R. Canahuire. Charlotte: Low-cost open-source semi-autonomous quadruped robot. In *2020 IEEE International Conference on Autonomous Robot Systems and Competitions (ICARSC)*, pages 281–286, April 2020.
- [12] Alexander Spröwitz, Alexandre Tuleu, Massimo Vespignani, Mostafa Ajallooeian, Emilie Badri, and Auke Jan Ijspeert. Towards dynamic trot gait locomotion: Design, control, and experiments with cheetah-cub, a compliant quadruped robot. *The International Journal of Robotics Research*, 32(8):932–950, 2013.
- [13] Tao Sun, Xiaofeng Xiong, Zhendong Dai, and Poramate Manoonpong. Small-sized reconfigurable quadruped robot with multiple sensory feedback for studying adaptive and versatile behaviors. *Frontiers in Neurorobotics*, 14:14, 2020.
- [14] F. Grimmerger, A. Meduri, M. Khadiv, J. Viereck, M. Wüthrich, M. Naveau, V. Berenz, S. Heim, F. Widmaier, T. Flayols, J. Fiene, A. Badri-Spröwitz, and L. Righetti. An open torque-controlled modular robot architecture for legged locomotion research. *IEEE Robotics and Automation Letters*, 5(2):3650–3657, April 2020.
- [15] Anqiao Li, Zhicheng Wang, Jun Wu, and Qiuguo Zhu. Bound controller for a quadruped robot using pre-fitting deep reinforcement learning, 2020.
- [16] DongHyun Ahn, Jae-Soon Lee, and Baek-Kyu Cho. Development of a quadruped jumpable robot pongbot-q. *The Journal of Korea Robotics Society*, 17(2):18–23, 2020.
- [17] J. Ramos, B. Katz, M. Y. M. Chuah, and S. Kim. Facilitating model-based control through software-hardware co-design. In *2018 IEEE International Conference on Robotics and Automation (ICRA)*, pages 566–572, May 2018.
- [18] G. Bledt, M. J. Powell, B. Katz, J. Di Carlo, P. M. Wensing, and S. Kim. Mit cheetah 3: Design and control of a robust, dynamic quadruped robot. In *2018 IEEE/RSJ International Conference on Intelligent Robots and Systems (IROS)*, pages 2245–2252, 2018.
- [19] Joonyoung Kim, Taewoong Kang, Dongwoon Song, and Seung-Joon Yi. Padwq open-source project repository. https://github.com/SJ-YI/PADWQ_open_source. accessed on 27 Mar 2021.
- [20] Y. Ding, A. Pandala, and H. Park. Real-time model predictive control for versatile dynamic motions in quadrupedal robots. In *2019 International Conference on Robotics and Automation (ICRA)*, pages 8484–8490, 2019.